ISBN: 978-3-95450-240-0 ISSN: 2673-5547 doi:10.18429/JACoW-HIAT2022-TH2I2

LONGITUDINAL BEAM DIAGNOSTICS R&D AT GSI-UNILAC

R. Singh*
GSI Helmholtzzentrum für Schwerionenforschung, Darmstadt, Germany

Abstract

GSI UNILAC provides a wide variety of ion types from energies ranging from 1.4 MeV/u to 11.5 MeV/u with a large dynamic range in the beam intensities to the experimental users or to the downstream accelerators. This flexibility in beam parameters requires a frequent tuning of the machine parameters for optimal operation of the UNILAC. Therefore, there has been a constant and pressing need for operationally convenient, accurate, fast and potentially non-destructive beam diagnostics for longitudinal charge profile and energy distribution. This contribution discusses the recent progress on longitudinal charge profile distribution measurements at GSI UNILAC. The outcome of recent devices like Fast Faraday cups (FFCs), transition radiation in GHz regime (GTR) is shown in comparison with phase probes or pick-ups. Other past developments aimed at longitudinal diagnostics at UNILAC like single particle detectors and RF deflector type methods are also briefly discussed.

INTRODUCTION

GSI Universal linear accelerator (UNILAC) is a complex set of resonators where detailed knowledge of longitudinal phase space is desired for optimizing the beam brilliance under flexible beam settings [1]. Past experiences suggest that the crucial locations for longitudinal phase determination is at the exit of High current injector (HSI), charge stripper sections and transfer channel to SIS-18. Figure 1 shows a schematic of the UNILAC where the various components of the UNILAC are shown along with the longitudinal diagnostics installations. Also marked is the measurement station X2 where most of the measurements discussed in this contribution were performed.

* r.singh@gsi.de

Longitudinal diagnostics are primarily concerned with the measurement of beam kinetic energy W_k, energy spread ($\delta = \Delta W_k/W_k$) and particle time/phase ($\Delta t/\Delta\phi$) of arrival spread with respect to the RF. Kinetic energy measurements are performed with Time of Flight (ToF) measurement between two or more phase probes (also referred as pick-ups/BPMs) and is routinely done at several locations along the UNILAC. The correlated distributions of beam energy spread and phase spread with respect to synchronous particle form an ellipse in longitudinal phase space. The area of the phase space ellipse is referred to as longitudinal emittance. The orientation of the ellipse at various accelerator locations can be controlled via bunchers and drifts. Typical strategy of determining full longitudinal phase space ellipse is by measuring one of the projection of longitudinal phase space) under various buncher settings and then performing tomographical reconstruction [2]. The measurement of phase/time of arrival spread also referred to as "longitudinal charge distribution" or loosely just "bunch length or bunch shape" is considered more accessible. The problem of longitudinal emittance determination is thus reduced to accurate measurement the longitudinal charge distribution. The devices used for longitudinal charge distribution is the main topic of this paper.

Longitudinal charge distribution measurements for relativistic charges ($\beta \approx 1$) or “long” charge distributions ($\Delta t \gg 1$ ns) is satisfactorily and non destructively performed using phase probes or wall current monitors until the electromagnetic design limitations. However, for UNILAC energies, i.e. $\beta < 0.15$ and the particle arrival time spread of about 0.4–2 ns (σ of a Gaussian distribution), the beam transverse field distribution is elongated significantly in comparison to charge distribution. This effect is here onward referred to as “field dilution”. Equation 1 shows the expression of the transverse field of a moving charge q with

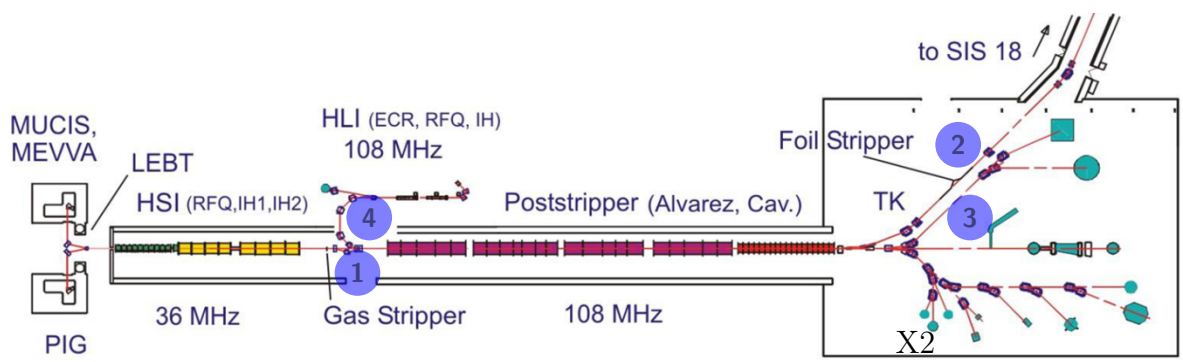

Figure 1: Schematic showing the UNILAC facility marking the location of various diagnostics. 1) Particle detectors 2) Dispersive section with RF deflector and screens 3) Gas Ionization BSM and 4) Feschenko BSM. R&D on FFC and GTR is ongoing in the area marked as “X2”.

ISBN: 978-3-95450-240-0 ISSN: 2673-5547 doi:10.18429/JACoW-HIAT2022-TH2I2

velocity βc at a distance R, which is the shortest perpendicular distance between charge propagation axis and phase probe.

$$E_T(R,\beta,t) = \frac{q}{4\pi\epsilon_0} \cdot \frac{\gamma R}{\left[R^2 + (\gamma\beta ct)^2\right]^{3/2}} \quad (1)$$

Figure 2 shows an example charge distribution and the corresponding transverse field at R = 30 mm for different charge velocities in accordance to Eq. (1). The dashed lines indicate the signal induced on the phase probe. The signal induction is based on the assumption that the contribution of phase probe to ground capacitance to the transfer impedance is negligible in the frequency range of interest.

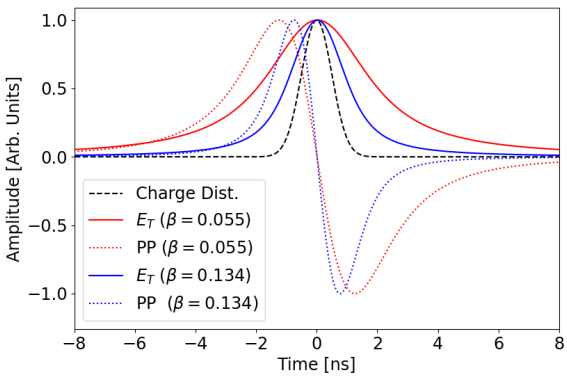

Figure 2: For the charge distribution (σ_t = 0.5 ns) showed by dashed lines, solid curves indicate the transverse field elongation for non-relativistic beam while dotted lines show the corresponding phase probe signal.

Figure 3 (top) shows 3 RF periods in a macropulse where charge distribution measured by a fast Faraday cup in comparison to the field distribution measured by a phase probe for 100 µA He^{1+} beam for the kinetic energy of 1.4 MeV/u ($\beta = 0.055$). The dotted lines mark the 108 MHz RF. The phase probe (PP) was located about ≈1 m upstream of the Faraday cup. Figure 3 (bottom) shows the averaged measurements over the full macropulse [3]. Also shown is the convolution of the FFC measurement with the analytical phase probe impulse response (Eq. (1)) which should ideally coincide with the phase probe measurement. The edges of the convolved signal are affected by the noise and it appears that the measured longitudinal charge distribution at FFC is smaller than the PP.

In the next section, alternate methods for longitudinal phase space determination historically used at UNILAC are discussed. Following that, recent R&D efforts on Fast Faraday cup measurements are discussed. Finally, a novel method for bunch length monitoring based on GHz transition radiation (GTR) is presented. The accuracy of FFC and GTR measurements are validated using simultaneous phase probe measurements.

BUNCH SHAPE MONITORS

Before the advent of fast oscilloscopes, two common approaches existed for charge distribution measurements for

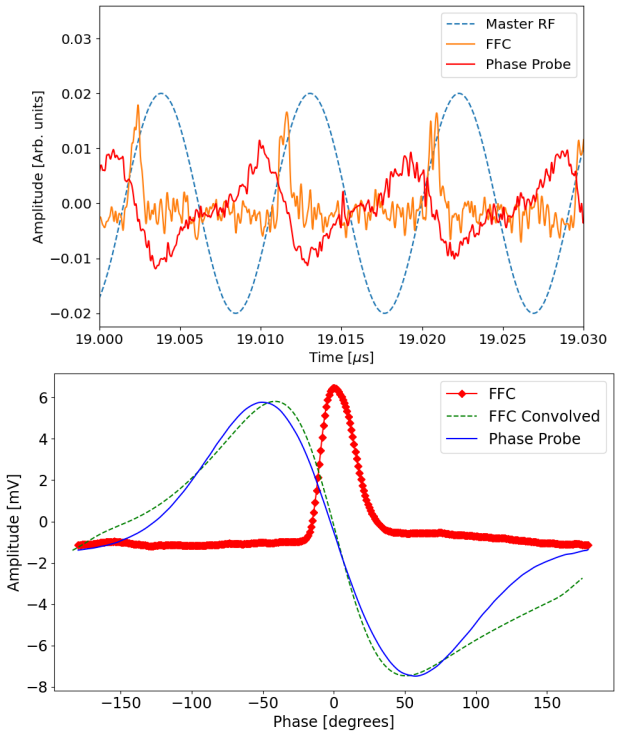

Figure 3: (Top) Snapshot of charge and field distribution measurements with FFC and PP within the macropulse. (Bottom) Averaged FFC and PP measurements along with convolution of FFC signal with impulse phase probe response.

non relativistic beams. The first one relies on scattering of the primary beam using a heavy metal foil (Tantalum, Gold etc.). The scattered beam is detected using charged particle detectors and time to digital converters (TDC) to measure particle time of arrival with respect to RF. At GSI, this principle is extended such that the scattered beam is detected twice, first via secondary electrons emitted from interaction with a thin aluminium foil followed by deposition in a diamond detector. This, in principle allowed for a simultaneous energy and phase spread measurements. The phase spread measurements were reliable while energy spread measurements were shown to be defective due to scattering foil non-uniformities. More details can be found here [4, 5] and references therein. Other facilities have used surface barrier detectors as charged particle detector with an otherwise similar principle [6].

Another commonly used method for bunch shape measurement is via generation of secondary electrons by irradiating a target material using primary beam. The low energy secondary electrons thus generated are carefully transported to a electron multiplier and a time to space conversion is performed in correlation with the master RF. The time-to-space conversion is performed via RF phase scan and slits or via the streak camera principle. Two devices, Feschenko BSM and Gas ionization based BSM which follow essentially the same principle described above, yet quite different realizations have been used at GSI. More details on these devices can be found here [5, 7] and references therein.

ISBN: 978-3-95450-240-0 ISSN: 2673-5547 doi:10.18429/JACoW-HIAT2022-TH2I2

FAST FARADAY CUPS

Fast Faraday cups are variants of the regular Faraday cups optimized for measuring fast time structures and not the beam current. The major challenges for accurate time structure of the beam using a Fast Faraday cup are

1. The FFC structure should be optimized for deposition of the charged particles and passing the induced signal until high frequencies. This includes matching to 50 Ω co-axial cables for signal transfer. The bandwidth of the system should be at least fives times the signal 3 dB cut-off in frequency domain i.e. $BW > \frac{5}{2\pi\Delta t}$
2. It should avoid the field dilution effects, i.e. measuring the preceding field of non-relativistic charges or it will encounter similar issues as with phase probes.
3. Suppress the distortion of induced signal due to secondary electron emission from the FFC collector. This is especially relevant for charged ion beams, since the number of secondary electrons scale with the charge state due to electronic stopping being the dominant mechanism.
4. Material damage to the FFC due to heating or melting of the cup under high intensity ion beams.

The problems listed above are known since the first Faraday cups were designed [8]. Earliest known design is an open ended tapered axially coupled co-axial structure [9, 10]. Currently, there is a repertoire of FFC designs based on modified co-axial cables and striplines. A front coupled stripline was used at SNS and Elettra [11] while a side coupled stripline was designed at BARC [12]. In this contribution, we will present the results of a radially coupled co-axial FFC obtained on loan from Fermilab.

The basic idea of this design is providing a blind hole from the side of a co-axial through the dielectric medium into the central conductor. The choice of hole width (1 mm) and depth (2 mm) is to minimize the escape of emitted secondary electrons. The blind hole in the central conductor of the co-axial is covered with a Titanium Zirconium Molybdenum Alloy (TZM) disk with a small 0.8 mm hole. The distance between TZM disk and the central conductor is optimized to reduce the field dilution effects. Detailed design is shown in Fig. 2 of this reference [13] along with further details. This device was successfully tested with low energy and low charge state beam and compared with a Feschenko monitor earlier [3]. In this contribution, beam with higher UNILAC energy and charge states was used for further validation measurements.

A 50 µs long Ar^{10+} beam macropulse with a kinetic energy of 8.6 MeV/u and 0.6 mA pulse current was measured at the FFC using 20 dB amplifier and 4 GHz, 40 GSa/s oscilloscope. Signal from a phase probe installed roughly 30 cm upstream was also simultaneously recorded using a comparable signal chain and acquisition electronics. The phase of one of the single gap resonators in the end section of UNILAC was utilized to vary the bunch shapes. Figure 4 shows the average bunch shape along with the phase probe signals for three buncher phase settings. A change in bunch shape is visible and interpreted as the defocusing of the beam at increased buncher phase settings. The detailed bunch shape evolution is shown in Fig. 5. From the bunch shape evolution, it appears that energy spread is not uniform and evolves along the macropulse.

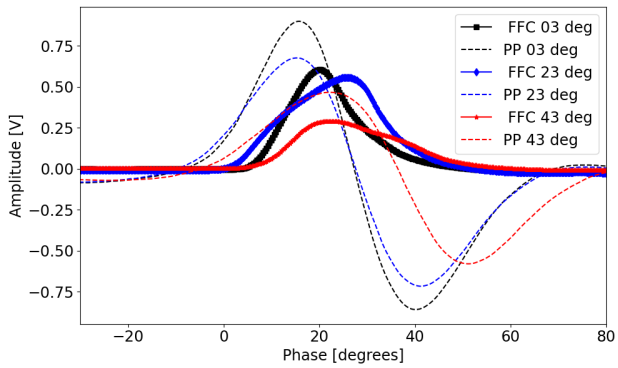

Figure 4: FFC bunch shape measurements with change in single gap resonator phase marked in the plot.

This bunch shape change along the macropulse is a general observation under various machine settings for moderate to high intensity beams in UNILAC and calls for "fast" measurements instead of "slow" averaged measurements.

Second validation measurement was performed by DC biasing of the FFC central conductor. This was performed to see the effect of secondary electrons emitted on the beam irradiation. This measurement was performed with 8.6 MeV/u 0.4 mA O^{6+} beam. Figure 6 shows a significant bunch "tail" of around 3ns is observed in the measured profile. The tail was suppressed on application of +ve bias and increased on application of –ve bias. Empirical estimates of secondary electron energy spectra suggest [14] that more than 90% electrons have energies below 30 eV and 30–50 V DC bias should be sufficient to suppress the signal distortion due to secondary emission. This measurement highlights the need of always positively biasing the central conductor when used with ion beams especially with higher charge states.

Another validation of the charge profile measured by FFC was performed by comparing it with the phase probe signal. Figure 7 shows the waterfall plot of the +25 V biased FFC and PP signal for the same macropulse.

While the FFC shows a phase/energy modulation along the macropulse, similar movement is not obvious in the PP signal. Figure 8 shows the comparison of the FFC signal convolved with PP impulse response and it appears that the FFC measured a reduced longitudinal charge profile in comparison to the PP. The potential reason is that, since the FFC is located in a dispersive section, it performs an energy selection of the beam through its 0.8 mm hole as depicted in Fig. 9.

This also makes it more sensitive to energy changes along the macropulse in comparison to the Phase probe. In nutshell, it should be emphasized that FFC should be placed in non-dispersive regions for trivial interpretation of its output. The signal obtained from FFCs placed in dispersive sections

ISBN: 978-3-95450-240-0 ISSN: 2673-5547 doi:10.18429/JACoW-HIAT2022-TH2I2

require a careful analysis and might even be useful scanning the phase space with FFC movement in the dispersive plane.

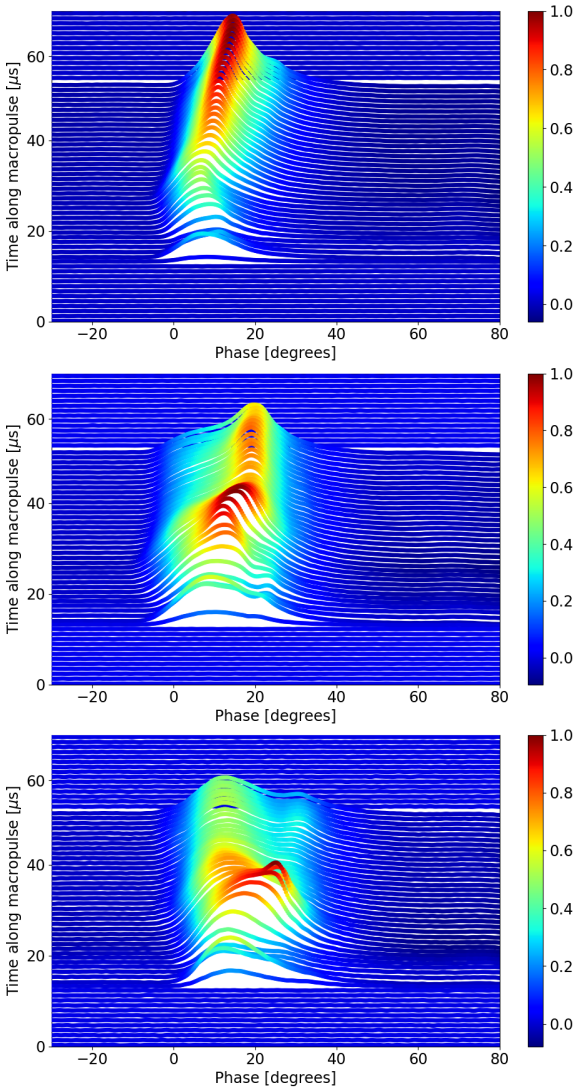

Figure 5: FFC bunch shape evolution for various single gap resonator phase (Top) 3 degrees, (Middle) 23 degrees and (Bottom) 43 degrees.

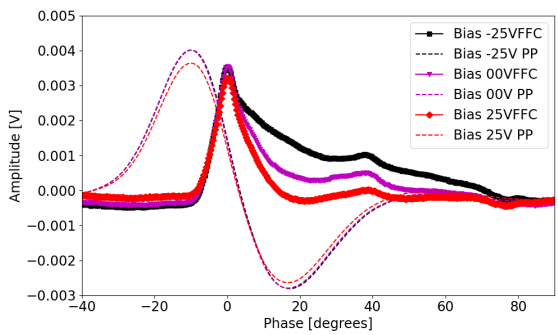

Figure 6: The longitudinal charge profile measurement averaged for a macropulse with application of various DC bias voltages on the FFC central conductor.

GHz TRANSITION RADIATION MONITOR

Transition radiation in GHz regime is coherent for sub-ns bunches. This frequency regime was utilized for bunch length measurements for the first time as reported earlier [15]. The E-Field of the coherent transition radiation for charge normally incident on a target in the far-field region is given as,

$$\vec{E}(t) = \frac{q\beta}{2\pi\epsilon_0 cR}\frac{\sin\theta\cdot\delta(R/c-t)}{1-\beta^2\cos^2\theta}\cdot(\hat{e}_x\cos\theta+\hat{e}_z\sin\theta) \quad (2)$$

R is the distance from the target center to the measurement location while θ is the angle between the target normal and measurement location in the plane of observation (refer Fig. 1 in [15]).

Detailed discussion on E-field analytical expressions in near field and corresponding CST simulations can be found

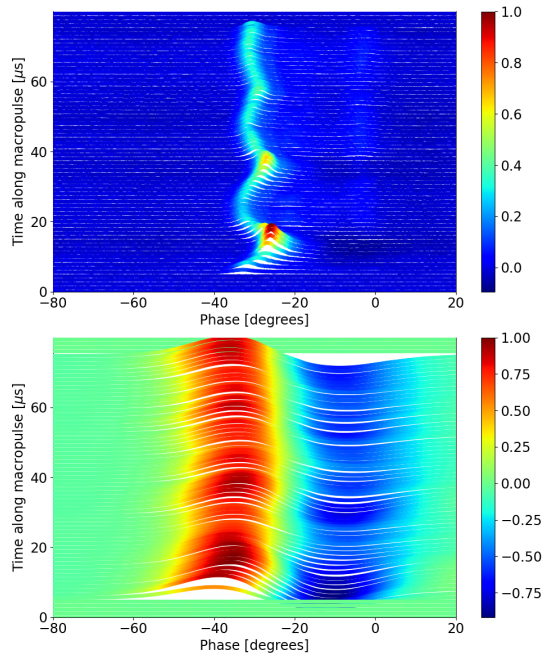

Figure 7: The waterfall plot showing the simultaneously recorded FFC and PP signal evolution along the macropulse. A phase modulation along the macropulse is visible.

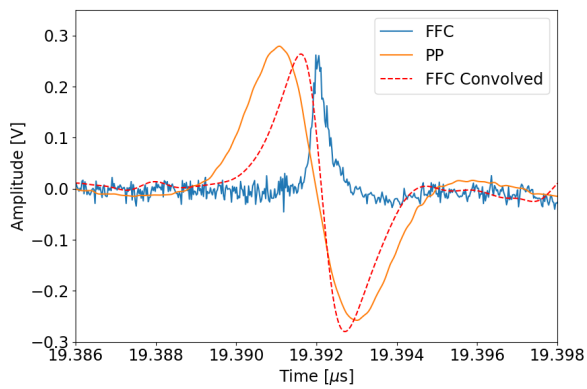

Figure 8: The FFC response convolved with the PP impulse response is much narrow in comparison to the PP signal.

ISBN: 978-3-95450-240-0 ISSN: 2673-5547 doi:10.18429/JACoW-HIAT2022-TH2I2

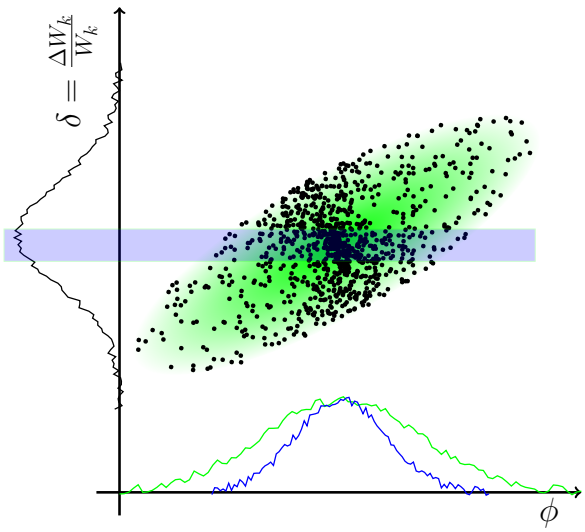

Figure 9: A schematic showing the effect of energy selection with dispersion on the measured bunch shape measured by the FFC.

here [15]. The radiation is polarized, broadband and proportional to the beam current. For 10 pC charge constrained in a 100 ps bunch, the peak measurable signal on a commercial biconical antenna is expected to be 10 mV. Other important concepts for transition radiation based measurements are the *effective source size* and radiation *formation zone*. *Effective source size* is the field elongation of the largest wavelength λ of interest and is given as, $\beta\gamma\lambda/2\pi$. The GTR target should at least be of this size in order not to cut-off useful lower frequencies required to reconstruct the bunch length via the radiated fields. Typically a small hole (10% of the effective source size) can be accommodated in the target for beam to go though without significantly affecting the induced radiation field. The *formation zone* is the area around the target where the radiation field is still transient. The radiation zone is generally dependent on the angle of radiation θ, however a simple yet conservative formula for the distance from target R which can be considered outside formation zone is given as $R = \gamma^2\lambda$. The measurement apparatus should be kept in the far field outside of the formation zone. The detailed consideration of all these concepts is discussed in [15].

The GTR measurement set-up is shown in Fig. 10. Prominent components include EM vacuum window made out of Quartz glass for the electromagnetic radiation to couple out of the vacuum and a Tantalum target with 3mm hole. There is a narrow tapered section to reject waveguide modes from leaving the beam pipe and interfere with the measurement device. A wideband biconical antenna (not shown) with a bandwidth of 4.5 GHz is placed at a distance of 1.0 m and 40 degrees with respect to beam axis from the target.

Figure 11 shows the bunch evolution in the macropulse measured by GTR and PP for 11.4 MeV/u Bi^{26+} with 0.4 mA average macropulse current. The trend in absolute signal strength and bunch shape is almost identical. The time of flight between PP and GTR monitor was also measured and matched to the expected beam velocity.

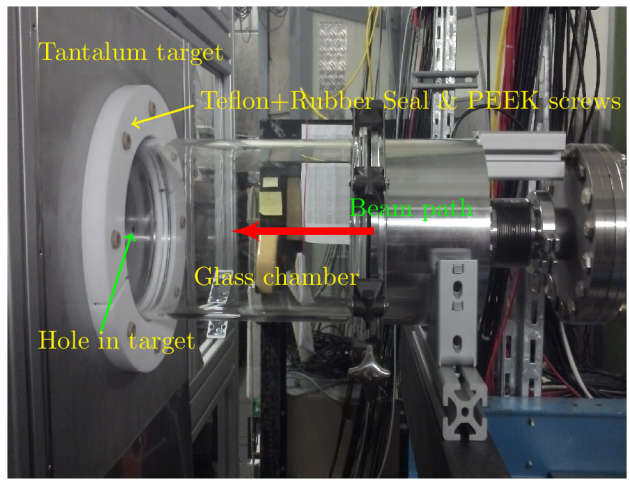

Figure 10: GTR measurements set-up

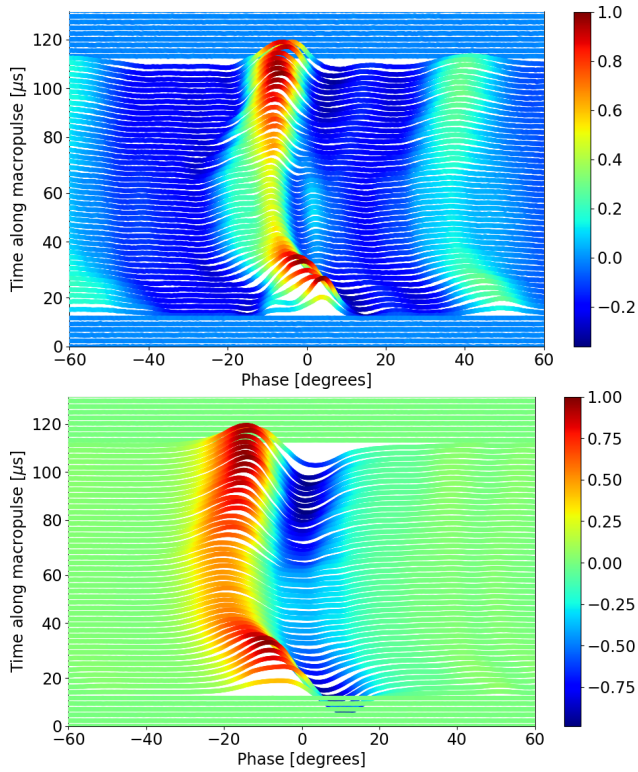

Figure 11: GTR and PP waterfall plot showing the bunch shape evolution along the macropulse.

In order to validate the accuracy of measured bunch shape by the GTR, the measured GTR signal was convolved with the analytical phase probe impulse response corresponding to $\beta = 0.154$ and compared with the phase probe signal. The outcome is shown in Fig. 12 and there is a good agreement between sampled phase space among the two devices. The wiggling behavior in the calculated convolution outside the bunch is due to enhancement of interferences by the convolution procedure. The various reflections from the glass window and metal parts in the measurement location are also visible and still pose a challenge for the GTR measurement.

ISBN: 978-3-95450-240-0 ISSN: 2673-5547 doi:10.18429/JACoW-HIAT2022-TH2I2

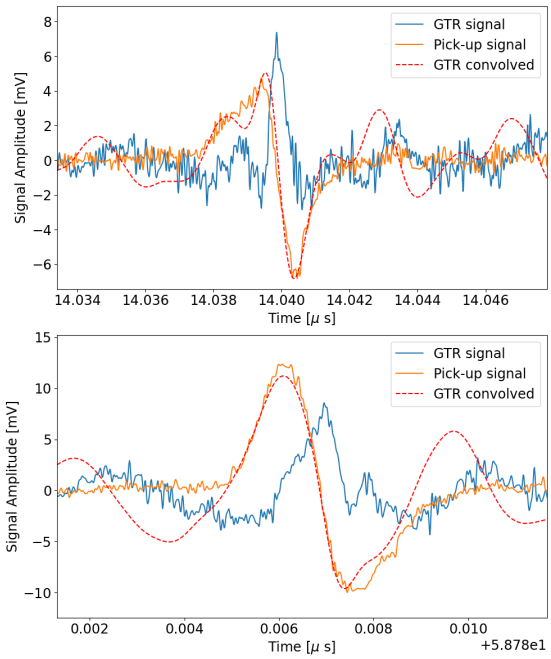

Figure 12: GTR signal along with its convolution through the PP response in comparison with the phase probe signal. A precise agreement between GTR and PP signal is seen.

CONCLUSION

The longitudinal charge distribution at UNILAC is seen to evolve within the macropulse in addition to pulse to pulse variation under moderate beam currents. These fast variations make the slower and established measurement options based on long averaging insufficient. Fast devices are therefore being sought and tested to obtain the longitudinal phase space and thus optimize the UNILAC. Based on the recent measurements, it was established that FFC is a compact and promising option and the central conductor should be biased with 30-50V. Further the FFC should be placed in a non-dispersive section to sample the complete phase space simultaneously and results should be validated against the phase probe signal. GTR monitor is a novel development and first results show precise agreement with the phase probe signal. It also allows non-invasive measurements of charge distribution which might be crucial for very high beam currents at high duty cycles.

ACKNOWLEDGEMENTS

The author would like to especially thank P. Forck and T. Reichert for many useful discussions and for providing DC biasing measurement data of the FFC. Colleagues from beam instrumentation, LINAC department and the machine operating team are gratefully acknowledged for the large support during this work on various aspects of installation and measurements. V. Scarpine, D. Sun and A. Shemyakin from FNAL for providing the FFC on loan as well as K. Mal and G. Rodrigues from IUAC for the simulation support of the FFC.

REFERENCES

[1] W. Barth *et al.*, "High brilliance beam investigations at universal linear accelerator", *Phys. Rev. Accel. Beams*, vol. 25, p. 040101, 2022. doi:10.1103/PhysRevAccelBeams.25.040101

[2] S. Lauber *et al.*, "Longitudinal phase space reconstruction for a heavy ion accelerator", *Phys. Rev. Accel. Beams*, vol. 23, p. 114201. doi:10.1103/PhysRevAccelBeams.23.114201

[3] R. Singh *et al.*, "Comparison of Feschenko BSM and Fast Faraday Cup with Low Energy Ion Beams", in *Proc. IBIC'21*, Pohang, Korea, Sep. 2021, pp. 407. doi:10.18429/JACoW-IBIC2021-WEPP16

[4] T. Milosic, "Feasibility Study on Longitudinal Phase-Space Measurements at GSI UNILAC using Charged-Particle Detectors", PhD. thesis, Technical University of Darmstadt, Germany, 2014. https://tuprints.ulb.tu-darmstadt.de/4321/1/Milosic_PhD-Thesis_2013.pdf

[5] P. Forck, "JUAS Lecture notes on beam instrumentation", 2021

[6] S. Ghosh *et al.*, "Method to reduce microphonics in superconducting resonators", *Phys. Rev. ST Accel. Beams*, vol. 10, p. 042002, 2007. doi:10.1103/PhysRevSTAB.10.042002

[7] B. Zwicker, "Design of a Bunch Shape Monitor for High Current LINACs at GSI", PhD thesis, University Frankfurt, 2016. https://www.gsi.de/fileadmin/SD/Theses/Thesis_DruckVersionDis_20160502.pdf

[8] J. M. Bogaty *et al.*, "A Very Wide Bandwidth Faraday Cup Suitable for Measuring Gigahertz Structure on Ion Beams with Velocities Down to $\beta < 0.01$", in *Proc. LINAC'90*, Albuquerque, NM, USA, Sep. 1990, pp. 465-467. https://jacow.org/l90/papers/tu457.pdf

[9] P. Strehl, "Beam instrumentation and diagnostics", Springer Berlin, Heidelberg, 2006. doi:10.1007/3-540-26404-3

[10] W. R. Rawnsley *et al.*, "Bunch shape measurements using fast Faraday cups and an oscilloscope operated by LabVIEW over Ethernet", *AIP Conference Proceedings*, vol. 546, p. 547, 2000. doi:10.1063/1.1342629

[11] M. Ferianis *et al.*, "Characterization of Fast Faraday cups at the ELETTRA LINAC", in *Proc. DIPAC'03*, Mainz, Germany, May 2003, pp. 113-115. https://jacow.org/d03/papers/PM10.pdf

[12] J. Matthew and A. Bajaj, "An improved strip-line fast Faraday cup for beam bunch measurements", *Review of Scientific Instruments*, vol. 91, p. 113305, 2020. doi:10.1063/5.0025457

[13] J.-P. Carniero *et al.*, "Longitudinal beam dynamics studies at the PIP-II injector test facility", *International Journal of Modern Physics A*, vol. 34, no. 36, 2019. doi:10.1142/S0217751X19420132

[14] A. Reiter *et al.*, "Investigation of Cross Talk in Secondary Electron Emission Grids", Technical Note LOBI-TN-SEM-2012-001, GSI, Darmstadt, 2012.

[15] R. Singh and T. Reichert, "Longitudinal charge distribution measurement of nonrelativistic ion beams using coherent transition radiation", *Phys. Rev. Accel. Beams*, vol. 25, p. 032801, 2022. doi:10.1103/PhysRevAccelBeams.25.032801